Helix−Loop−Helix Peptides as Scaffolds for the Construction of Bridged Metal Assemblies in Proteins: The Spectroscopic A-Cluster Structure in Carbon Monoxide Dehydrogenase

Catalina E. Laplaza and R. H. Holm*

Contribution from the Department of Chemistry and Chemical Biology, Harvard University, Cambridge, Massachusetts 02138

Received April 2, 2001

Abstract: Four helix−loop−helix 63mer peptides were designed and synthesized in order to assess the utility of peptides as scaffolds for the stabilization of complex metal sites in proteins. Bridged assembly [Ni^{II}−(μ_2-S·Cys)−Fe_4S_4], consistent with spectroscopic information on the A-cluster of carbon monoxide dehydrogenase, was chosen as the target assembly. The peptides consist of two helices with ∼20 residues connected by a flexible loop containing the ferredoxin consensus sequence Cys-Ile-Ala-Cys-Gly-Ala-Cys to bind the Fe_4S_4 cluster. A fourth cysteine was positioned to serve as the bridging ligand between the cluster and Ni(II). Three other binding residues were incorporated in appropriate positions to constitute a binding site for Ni(II). One of the peptides was designed with an N_3S (His_3Cys) site, and each of the other three with N_2S_2 (His_2Cys_2) sites. A detailed account of the synthesis and characterization of the peptides and their metalloderivatives is presented. The four peptides were synthesized using an Fmoc/*t*-Bu-based solid-phase strategy, purified by reversed-phase HPLC, and characterized by ES-MS. On the basis of size-exclusion chromatography and circular dichroism spectropolarimetry, these peptides appear to dimerize in solution to form four-helix bundles of high helical contents. Reactions of the peptides with preformed cluster $[Fe_4S_4(SCH_2CH_2OH)_4]^{2-}$ and subsequent purification by column chromatography yield a product consistent with the incorporation of one $[Fe_4S_4]^{2+}$ cluster per 63mer, as judged from absorption and Mössbauer spectra. Addition of a Ni(II) salt to the $[Fe_4S_4]$− peptides results in an apparent equilibrium between free Ni(II) and a peptide-bound nickel form, as established by column chromatography studies. Nickel EXAFS data (Musgrave, K. B.; Laplaza, C. E.; Holm, R. H.; Hedman, B.; Hodgson, K. O. Results to be published.) provide strong evidence that the peptide-bound nickel binds in the desired site in two of the metallopeptides. This work represents the first exploration of peptides as scaffolds for the support of biologically relevant bridged assemblies containing iron−sulfur clusters.

Introduction

In recent years, a large number of metallopeptides have been designed and synthesized for a variety of purposes. Among the more common motives are studies of interactions with nucleic acids,[1,2] long-range electron transfer,[3−7] the nucleation and stabilization of α-helices and β-sheets,[8−10] and the construction of structural analogues of the active sites of metalloproteins. The latter include, inter alia, zinc proteins,[9,11,12] heme proteins,[7] and, of particular pertinence to this research, iron−sulfur proteins with Fe_4S_4 clusters.[4,13−20] An excellent example of the use of de novo designed peptides to stabilize protein-bound sites is the recent work by DeGrado and co-workers.[21] Here, the design of metallopeptides is directed toward the stabilization of two-iron sites based on a retrostructural analysis of primary ligands and second-shell interactions in proteins with binuclear sites. As also pointed out by Hill et al.,[10] other approaches for mimicking active sites of enzymes include the use of flexible peptides that wrap around the metal site by folding into secondary and tertiary structures and the selective mutation of

(1) Long, E. C. *Acc. Chem. Res.* **1999**, *32*, 827−836.
(2) Nagane, R.; Koshigoe, T.; Chikira, M.; Long, E. C. *J. Inorg. Biochem.* **2001**, *83*, 17−23.
(3) Mutz, M. W.; Case, M. A.; Wishart, J. F.; Ghadiri, M. R.; McLendon, G. L. *J. Am. Chem. Soc.* **1999**, *121*, 858−859.
(4) Gibney, B. R.; Mulholland, S. E.; Rabanal, F.; Dutton, P. L. *Proc. Natl. Acad. Sci. U.S.A.* **1996**, *93*, 15041−15046.
(5) Rau, H. K.; Haehnel, W. *J. Am. Chem. Soc.* **1998**, *120*, 468−476.
(6) Kornilova, A. Y.; Wishart, J. F.; Xiao, W.; Lasey, R. C.; Fedorova, A.; Shin, Y.-K.; Ogawa, M. Y. *J. Am. Chem. Soc.* **2000**, *122*, 7999−8006.
(7) Gibney, B. R.; Dutton, P. L. *Adv. Inorg. Chem.* **2001**, *51*, 409−455.
(8) Schneider, J. P.; Kelly, J. W. *Chem. Rev.* **1995**, *95*, 2169−2187.
(9) DeGrado, W. F.; Summa, C. M.; Pavone, V.; Nastri, F.; Lombardi, A. *Annu. Rev. Biochem.* **1999**, *68*, 779−819.
(10) Hill, R. B.; Raleigh, D. P.; Lombardi, A.; DeGrado, W. F. *Acc. Chem. Res.* **2000**, *33*, 745−754.
(11) Berg, J. M.; Godwin, H. A. *Annu. Rev. Biophys. Biomol. Struct.* **1997**, *26*, 357−371.
(12) Hori, Y.; Suzuki, K.; Okuno, Y.; Nagaoka, M.; Futaki, S.; Sugiura, Y. *J. Am. Chem. Soc.* **2000**, *122*, 7648−7653.
(13) Smith, E. T.; Feinberg, B. A.; Richards, J. H.; Tomich, J. M. *J. Am. Chem. Soc.* **1991**, *113*, 688−689.
(14) Smith, E. T.; Tomich, J. M.; Iwamoto, T.; Richards, J. H.; Mao, Y.; Feinberg, B. A. *Biochemistry* **1991**, *30*, 11669−11676.
(15) Sow, T.-C.; Pedersen, M. V.; Christensen, H. E. M.; Ooi, B.-L. *Biochem. Biophys. Res. Commun.* **1996**, *223*, 360−364.
(16) Feinberg, B. A.; Lo, X.; Iwamoto, T.; Tomich, J. M. *Protein Eng.* **1997**, *10*, 69−75.
(17) Scott, M. P.; Biggins, J. *Protein Sci.* **1997**, *6*, 340−346.
(18) Coldren, C. D.; Hellinga, H. W.; Caradonna, J. P. *Proc. Natl. Acad. Sci. U.S.A.* **1997**, *94*, 6635−6640.
(19) Mulholland, S. E.; Gibney, B. R.; Rabanal, F.; Dutton, P. L. *J. Am. Chem. Soc.* **1998**, *120*, 10296−10302.
(20) Mulholland, S. E.; Gibney, B. R.; Rabanal, F.; Dutton, P. L. *Biochemistry* **1999**, *38*, 10442−10448.
(21) Lombardi, A.; Summa, C. M.; Geremia, S.; Randaccio, L.; Pavone, V.; DeGrado, W. F. *Proc. Natl. Acad. Sci. U.S.A.* **2000**, *97*, 6298−6305.

10.1021/ja010851m CCC: $20.00
Published on Web 09/28/2001

certain amino acids from the sequence of a protein with known structure to integrate a metal site absent in the natural protein.

Of particular interest to us is the use of de novo designed peptides as metal scaffolds for the formation and stabilization of structural analogues of the more complex metal sites found in biology, which we have termed "bridged biological assemblies".[22] These consist of two discrete fragments that are juxtaposed wholly or in part by one or more covalent bridges. Examples include the [heme−(μ_2-S·Cys)−Fe_4S_4] site in sulfite reductase[23] and the heme−a_3−Cu_B substructure of cytochrome *c* oxidase, which is reported to be peroxide-bridged in the resting form.[24,25] The use of traditional organic ligands for stabilizing bridged assemblies is conceivable but problematic, given the spatial and metric demands inherent in the design for a given assembly and the potentially lengthy synthesis involved. Further, a misdesigned ligand may require a different synthetic approach. In the context of stabilizing bridged assemblies, designed peptides offer several advantages: (i) certain amino acid sequences fold into specific secondary and tertiary structures, which could afford correct spatial positioning of the components of an assembly; (ii) automated peptide synthesis facilitates addition, deletion, and mutation of residues, even for large peptides, in the event that a sequence design is found to be flawed or that a variation in ligands and/or geometry is desired; (iii) coordinating ligands are physiological in nature; (iv) solvent accessibility to the metal center can be modulated by the number of hydrophobic interactions between the amino acids that fold around the metal site; and (v) aqueous solubility can be promoted by appropriate inclusion of hydrophilic residues.

Examples of bridged structures that are difficult to stabilize using traditional organic ligands can be found in the proposed structures of the two active sites, the A-cluster and the C-cluster, of the bifunctional enzyme carbon monoxide dehydrogenase (CODH).[26] A high-resolution X-ray structure of this enzyme is not currently available. The A-cluster, which is involved in the last step of the synthesis of acetyl-CoA, has been proposed to be a bridged assembly [Ni−X−Fe_4S_4] in which bridging atom or group X is presently unidentified. Evidence for the bridge derives from EPR,[27,28] ENDOR,[29] and Mössbauer[28,30] studies. Nickel EXAFS data analysis suggests that the nickel atom binds two S ligands and two N/O ligands in a distorted square planar arrangement.[31] In the oxidized form, the nickel atom appears to exist as low-spin Ni(II).[28,32] The C−cluster, where CO is reversibly oxidized to CO_2, exhibits ENDOR[33] and Mössbauer[34] spectroscopic features also consistent with an assembly [Ni−X−Fe_4S_4]. EXAFS results point to a nickel atom with two S ligands and two to three N/O ligands in a tetrahedral or distorted five-coordinate geometry.[35] The synthetic cluster closest in structure to center A is $[LNiFe_4S_4I_3]^{1-}$, in which Ni(II) is covalently linked through *two* thiolate bridges of tetradentate ligand L to a single iron atom of the Fe_4S_4 cluster.[36]

We have chosen the proposed A-cluster of CODH to test the use of peptides as metal scaffolds for the formation and stabilization of structural analogues of a bridged assembly. At the outset, we note certain pertinent results in Fe_4S_4−peptide chemistry. Sow et al.[15] synthesized a 31-residue Fe_4S_4 miniferredoxin, whose design was based on the known structure of the 58-residue *D. gigas* Fe_3S_4 ferredoxin II, by selectively mutating and deleting certain residues. To mimick the F_x-cluster in Photosystem I, Scott and Biggins[17] incorporated the Fe_4S_4 cluster into a variant of a four α-helix bundle designed by Regan and DeGrado.[37] The Fe_4S_4 cluster has been introduced by Caradonna and co-workers[18] into the protein frame of thioredoxin after mutation of several key residues, according to the protein design algorithm DEZYMER. These results demonstrate that Fe_4S_4 clusters can be stabilized in non-native protein environments. Even more relevant to the present work, Gibney et al.[4] successfully incorporated the Fe_4S_4 cluster into a 16-residue random coil peptide and into a 67-residue helix−loop−helix peptide, both of which contained a ferredoxin consensus sequence. Furthermore, they have performed several mutations within the consensus sequence to determine which amino acids are the most important for the incorporation of the cluster.[19,20] As discussed below, we have chosen the same ferredoxin consensus sequence for the incorporation of the Fe_4S_4 cluster into the loops of helix−loop−helix peptides with 63 residues. The work described here is the starting point of our investigation of designed peptides as scaffolds for complex metal sites, the proposed bridged assembly for the CODH A-cluster.

Experimental Section

Materials. All amino acids, the resin Fmoc-PAL-PEG-PS (0.17−0.18 mmol/g), HATU (*N*-[dimethylamino-1*H*-1,2,3-triazol[4,5-b]pyridin-1-ylmethylene]-*N*-methylmethanaminium hexafluorophosphate *N*-oxide), 20% piperidine in DMF, diisopropylethylamine (DIEA), and acetic anhydride were purchased from Applied Biosystems. The following materials were obtained from the indicated sources: thioanisole, 1,2-ethanedithiol (EDT), 2-mercaptoethanol, $NiCl_2·6H_2O$, and (*R*)-(−)-pantolactone from Aldrich; $Ni(BF_4)_2·6H_2O$ from Strem; phenol, dichloromethane (DCM), and NaCl from Mallinckrodt; *N*,*N*′-dimethylformamide (DMF) and trifluoroacetic acid (TFA) from EM Science; *N*-methyl-pyrrolidone (NMP), Tris base, and Tris hydrochloride from J. T. Baker; dithiothreitol (DTT) from Alfa AESAR; Sephadex G-25 medium from Amersham Pharmacia Biotech; ultrapure $(NH_4)_2SO_4$ from ICN Biomedicals, Inc.; ^{57}Fe (94.7% enriched) from Penwood Chemicals. The side-chain protecting groups on the amino acids were trityl for cysteine and histidine, *t*-Boc for lysine, and O-*t*-Bu for glutamic acid. $(Me_4N)_2[Fe_4S_4(SCH_2CH_2OH)_4]$ was prepared according to the literature procedure.[38,39]

(22) Holm, R. H. *Pure Appl. Chem.* **1995**, *67*, 217−224.
(23) Crane, B. R.; Siegel, L. M.; Getzoff, E. D. *Science* **1995**, *270*, 59−67.
(24) Yoshikawa, S.; Shinzawa-Itoh, K.; Nakashima, R.; Yaono, R.; Yamashita, E.; Inoue, N.; Yao, M.; Fei, M. J.; Libeu, C. P.; Mizushima, T.; Yamaguchi, H.; Tomizaki, T.; Tsukihara, T. *Science* **1998**, *280*, 1723−1729.
(25) Yoshikawa, S.; Shinzawa-Itoh, K.; Tsukihara, T. The Structure of Bovine Heart Cytochrome *c* Oxidase; In *Frontiers of Cellular Bioenergetics*; Papa, S., Guerrieri, F., Tager, J. M., Eds.; Kluwer Academic/Plenum Publishers: New York, 1999; pp 131−156.
(26) Ragsdale, S. W.; Kumar, M. *Chem. Rev.* **1996**, *96*, 2515−2539.
(27) Xia, J.; Lindahl, P. A. *J. Am. Chem. Soc.* **1996**, *118*, 483−484.
(28) Xia, J.; Hu, Z.; Popescu, C. V.; Lindahl, P. A.; Münck, E. *J. Am. Chem. Soc.* **1997**, *119*, 8301−8312.
(29) Fan, C.; Gorst, C. M.; Ragsdale, S. W.; Hoffman, B. M. *Biochemistry* **1991**, *30*, 431−435.
(30) Lindahl, P. A.; Ragsdale, S. W.; Münck, E. *J. Biol. Chem.* **1990**, *265*, 3880−3888.
(31) Xia, J.; Dong, J.; Wang, S.; Scott, R. A.; Lindahl, P. A. *J. Am. Chem. Soc.* **1995**, *117*, 7065−7070.
(32) Ralston, C. Y.; Wang, H.; Ragsdale, S. W.; Kumar, M.; Spangler, N. J.; Ludden, P. W.; Gu, W.; Jones, R. M.; Patil, D. S.; Cramer, S. P. *J. Am. Chem. Soc.* **2000**, *122*, 10553−10560.
(33) DeRose, V. J.; Telser, J.; Anderson, M. E.; Lindahl, P. A.; Hoffman, B. M. *J. Am. Chem. Soc.* **1998**, *120*, 8767−8776.
(34) Hu, Z.; Spangler, N. J.; Anderson, M. E.; Xia, J.; Ludden, P. W.; Lindahl, P. A.; Münck, E. *J. Am. Chem. Soc.* **1996**, *118*, 830−845.
(35) Tan, G. O.; Ensign, S. A.; Ciurli, S.; Scott, M. J.; Hedman, B.; Holm, R. H.; Ludden, P. W.; Korszun, Z. R.; Stephens, P. J.; Hodgson, K. O. *Proc. Natl. Acad. Sci. U.S.A.* **1992**, *89*, 4427−4431.
(36) Osterloh, F.; Saak, W.; Haase, D.; Pohl, S. *J. Chem. Soc., Chem. Commun.* **1996**, 777−778.
(37) Regan, L.; DeGrado, W. F. *Science* **1988**, *241*, 976−978.
(38) Hill, C. L.; Renaud, J.; Holm, R. H.; Mortenson, L. E. *J. Am. Chem. Soc.* **1977**, *99*, 2549−2557.
(39) Christou, G.; Garner, C. D. *J. Chem. Soc., Dalton Trans.* **1979**, 1093−1094.

Peptide Synthesis and Purification. Peptides with 63 residues (63mers) were assembled in the PE Biosystems Pioneer Peptide Synthesis System using an Fmoc/*t*-Bu-based strategy with magic mixture solvent[40] at a 0.1 mmol scale. The protocol for the synthesis of 63mers is summarized in Figure 1; the four product peptides are specified in Figure 2 together with their designations. The synthesis of HC_4H_2 has been described elsewhere;[41] here we give a more detailed procedure. N^{α}-Fmoc removal was accomplished via treatment with a solution of 1% Triton X-100 (reduced) in piperidine−DMF−NMP (1:2:2) for 10 min; acylation was carried out for 1 h with HATU/DIEA in 1% Triton X-100 (reduced) and 2 M ethylene carbonate in DCM−DMF−NMP (3:3:1). Additionally, the last 38 couplings were heated at 55 °C by wrapping the reaction column with heating tape. The N-terminus was acetylated with 20% acetic anhydride in DCM for 1 h. The peptide was cleaved from the resin, and the side chains were deprotected upon treatment with TFA−phenol−H_2O−thioanisole−EDT (82.5:5:5:5:2.5 v/v). In a typical cleavage and side chain deprotection procedure, the peptide−resin (500−600 mg) was stirred in 20 mL of the above cleavage cocktail for 1.5 h. The reaction mixture was filtered, and the beads were washed with 10 mL of TFA. The combined filtrates were divided equally between twelve 50 mL polypropylene centrifuge tubes, each containing 40 mL of cold ether (−20 °C). The precipitated peptide was centrifuged. Finally, the isolated peptide in each tube was washed three times with 45 mL of ether and dried under a stream of N_2. Purification of the peptides was achieved by reversed-phase C_{18} HPLC in a Rainin Dynamax instrument equipped with a YMC 120 Å semipreparative column. Linear gradients over 15 min of CH_3CN/0.1% TFA in H_2O/0.1% TFA were run at a flow rate of 24.9 mL/min from 39 to 60% for the peptide HC_4H_2, 40 to 65% for HC_4HC, 39 to 63% for HC_5H, and 38 to 63% for CHC_4H while monitoring the absorbance at 214 nm. A typical preparation of a sample to be purified in this manner consisted of dissolving every 20 mg of crude peptide in 1 mL of water containing 5 mg of DTT, filtering the resulting mixture through an acrodisc, and heating the solution at ∼80 °C for 1−2 min.

Electrospray Mass Spectrometry. ES-MS spectra were recorded on a Platform 2 mass spectrometer (Micromass Instruments, Danvers, MA) or on an LCT mass spectrometer (Micromass Instruments, Danvers, MA). All spectra exhibited the expected ion peaks and the expected deconvoluted molecular weight spectrum as described below.

(a) HC_4H_2 *m*/*z*, found (calcd): $z = 6$, 1257 (1257); $z = 7$, 1077 (1078); $z = 8$, 943 (943); $z = 9$, 838 (838); $z = 10$, 755 (755); $z = 11$, 686 (686); $z = 12$, 629 (629); $z = 13$, 581 (581). Found [M]: 7536, through deconvolution. Calcd [M]: 7537.

(b) HC_4HC *m*/*z*, found (calcd): $z = 4$, 1875 (1876); $z = 5$, 1501 (1501); $z = 6$, 1251 (1251); $z = 7$, 1072 (1072); $z = 8$, 938 (938); $z = 9$, 834 (834); $z = 10$, 751 (751). Found [M]: 7498, through deconvolution. Calcd [M]: 7498.

(c) HC_5H *m*/*z*, found (calcd): $z = 5$, 1502 (1501); $z = 6$, 1251 (1251); $z = 7$, 1073 (1072); $z = 8$, 939 (938); $z = 9$, 835 (834); $z = 10$, 751 (751). Found [M]: 7496, through deconvolution. Calcd [M]: 7498.

(d) CHC_4H *m*/*z*, found (calcd): $z = 5$, 1501 (1501); $z = 6$, 1251 (1251); $z = 7$, 1072 (1072); $z = 8$, 938 (938); $z = 9$, 834 (834); $z = 10$, 751 (751); $z = 11$, 683 (683); $z = 12$, 626 (626). Found [M]: 7499, through deconvolution. Calcd [M]: 7498.

Determination of Peptide Concentrations. Peptide concentrations were determined spectrophotometrically on the basis of the contribution of Phe at 259 nm and by using $\epsilon_{259} = 195\ M^{-1}\ cm^{-1}$.[42] Because several components of this peptide absorb at 259 nm, it was necessary to deconvolute the UV spectrum as follows. Data points in the 350−370 nm region were fitted to a line by the least-squares method to obtain the absorption equation due to light scattering arising from haze in the solution,[43] which was then subtracted from the original UV spectrum.

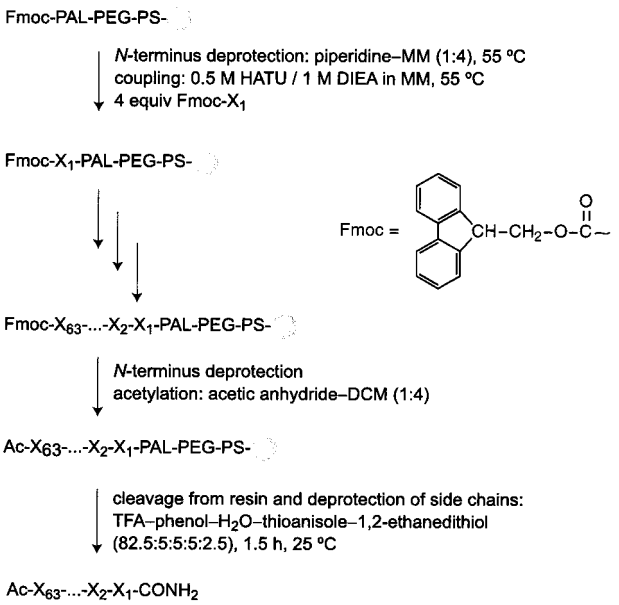

Figure 1. Synthetic scheme for the 63mer peptides. X = amino acid residue. Magic mixture[40] (MM) for couplings = DMF−DCM−NMP (3:3:1), 1% triton X-100 (reduced), 2 M ethylene carbonate; magic mixture[40] (MM) for *N*-terminus deprotection = DMF−NMP (1:1), 1% triton X-100 (reduced).

The program Kaleidagraph was then used to fit the resulting spectrum in the 235−370 nm range to the equation $y = m_1 \exp[-(214 - x)^2/m_2] + m_3\{\exp[-(259 - x)^2/6.8] + 0.81 \exp[-(253 - x)^2/25] + 1.2 \exp[-(265 - x)^2/29)] + 0.81 \exp[-(249 - x)^2/227]\} + m_4 \exp[-(249 - x)^2/1300] + m_5$, where m_1 is the maximum absorbance of the Gaussian distribution from amide bonds with A_{max} at 214 nm, m_2 is a variable correlating to the width at half-height of the amide bonds' absorbance by the equation width $= 2(m_2 \ln 2)^{1/2}$, m_3 is a variable correlating to the concentration of Phe, m_4 is the maximum absorbance of the Gaussian distribution from cystines with A_{max} at 249 nm and with a width at half-height of 60 nm, and $m5$ is the baseline. Unlike the absorbance contributions arising from amide bonds and cystines, those from Phe cannot be fitted properly using a Gaussian distribution expression. To obtain a more adequate approximation of the absorbance of Phe that takes into account its non-Gaussian shape and fine structure, its UV spectrum was recorded and analyzed with Kaleidagraph. Given the limitations of the program (9 variables maximum), the best representation of the Phe absorbance was determined to be given by the expression $[\exp(-(259 - x)^2/6.8) + 0.81 \exp(-(253 - x)^2/25) + 1.2 \exp(-(265 - x)^2/29) + 0.81 \exp(-(249 - x)^2/227)]$, which is the sum of four Gaussian components of different heights and widths. As seen above, this expression was integrated into the equation for the deconvolution of the UV spectra of peptide solutions. The simpler procedure of incorporating Trp into the sequences was not employed in order to allow detection of any UV bands of the metal chromophores.

Fe_4S_4 Incorporation into 63mer Peptides from Preformed Cluster $[Fe_4S_4(SCH_2CH_2OH)_4]^{2-}$. Incorporation of the Fe_4S_4 cluster into each one of the 63mer peptides was achieved by a slightly modified literature procedure[18] illustrated with the following typical preparation of HC_5H−$[Fe_4S_4]$. Under a dinitrogen atmosphere, the peptide HC_5H (19.9 mg, 2.65 μmol) was dissolved in 5.91 mL of Tris buffer (50 mM, pH 8.0, 0.1 M NaCl) and its concentration determined as described above to be 372 μM. This solution was then made to be 2% v/v in 2-mercaptoethanol. After allowing this mixture to stand for 2 h to reduce any disulfide bonds, 600 μL of a freshly prepared 8.8 mM solution of $(Me_4N)_2[Fe_4S_4(SCH_2CH_2OH)_4]$ in the Tris buffer solution was added. The resulting yellow-brown reaction mixture (330 μM in peptide, 800 μM in $(Me_4N)_2[Fe_4S_4(SCH_2CH_2OH)_4]$) was left overnight to ensure reaction completion. The excess reagents were removed by eluting the

(40) Zhang, L.; Goldammer, C.; Henkel, B.; Zühl, F.; Panhaus, G.; Jung, G.; Bayer, E. In *Innovation and Perspective in Solid-Phase Synthesis*; Epton, R., Ed.; Mayflower: Birmingham, U.K., 1994; pp 711−716.

(41) Laplaza, C. E.; McNamara, J. F.; Kates, S. A.; Holm, R. H. In *Peptides 1998*; Bajusz, S., Hudecz, F., Eds.; Akadémiai Kiadó: Budapest, 1999; pp 320−321.

(42) *CRC Handbook of Biochemistry*; Chemical Rubber Co.: Cleveland, OH, 1970; p B76.

(43) Beaven, G. H.; Holiday, E. R. *Adv. Protein Chem.* **1952**, *7*, 319−386.

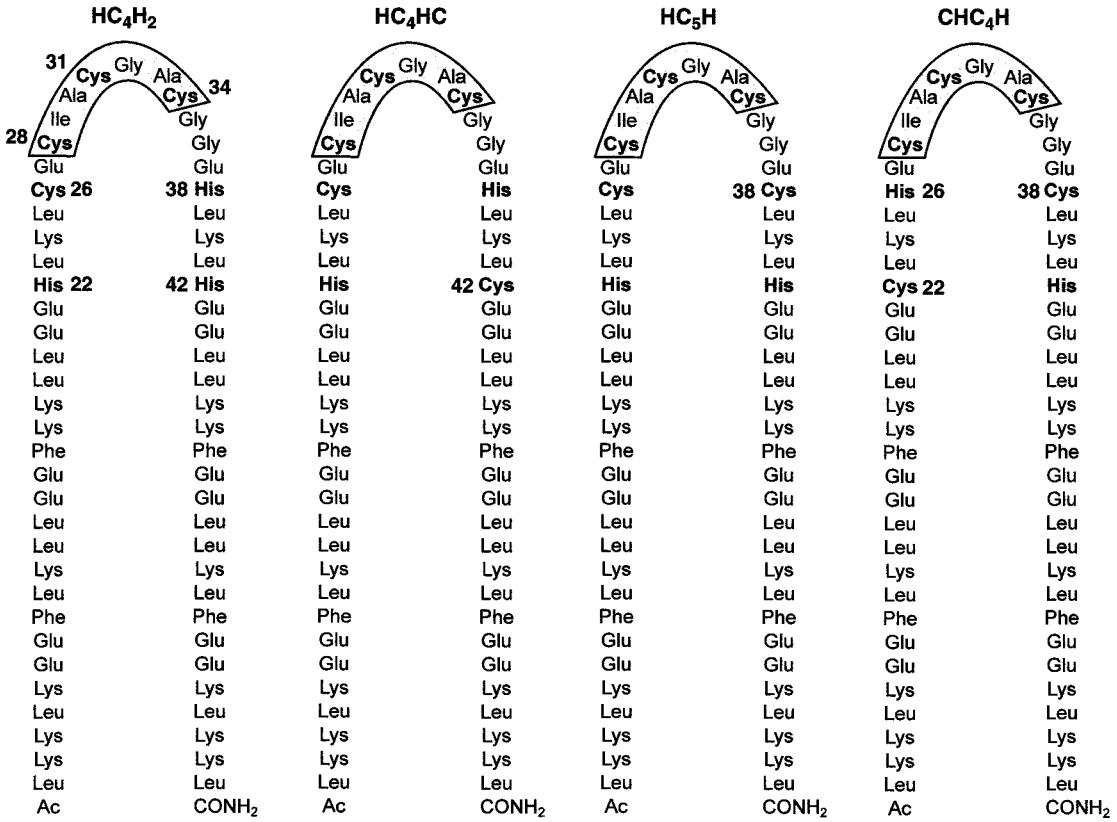

Figure 2. Sequences of 63mer peptides designed to encapsulate the bridged assembly $[Ni^{II}-(\mu_2\text{-}S\cdot Cys)-Fe_4S_4]$.

reaction mixture through a Sephadex G-25 column (6.5 cm × 3 cm). The absorption spectrum of the collected brown fraction showed the presence of two bands, at 290 and 380 nm, characteristic of an $[Fe_4S_4]^{2+}$ cluster.[38] Under the assumptions that all iron detected by atomic absorption is in the form of Fe_4S_4 and that all peptide is recovered after elution through the Sephadex column, incorporation yields of 85−95% have been obtained by this procedure.

Nickel(II) Incorporation into 63mer−[Fe_4S_4] Peptides. One equiv of $NiCl_2\cdot 6H_2O$ or $Ni(BF_4)_2\cdot 6H_2O$ was added to a solution of each 63mer−$[Fe_4S_4]$ in Tris buffer (50 mM, pH 8.0, 0.1 M NaCl) and allowed to react overnight, after which each reaction mixture was eluted through a Sephadex G-25 column. A UV−vis spectrum of each eluant was collected to corroborate that the $[Fe_4S_4]^{2+}$ cluster was not destroyed. The ratios Ni:Fe were determined through atomic absorption spectroscopy.

Size-Exclusion Chromatography. To estimate the molecular weight of each 63mer peptide and metallopeptide in solution, size-exclusion chromatography (SEC) was performed inside an argon glovebag with a Rainin Dynamax instrument equipped with a Pharmacia Biotech Superdex 75 10/30 size-exclusion column (300 mm × 10 mm) equilibrated with 50 mM Tris buffer, pH 8.0, containing 0.1 M NaCl. To calibrate the column, the following standards obtained from Bio-Rad Laboratories were used: chicken ovalbumin (44 kDa), horse myoglobin (17 kDa), and vitamin B_{12} (1.35 kDa). All runs were performed at a flow rate of 0.5 mL/min. The elution of the standards and the 63mer peptides was monitored at 220 nm, while the metallopeptides were followed at 380 nm.

Circular Dichroism Spectropolarimetry. CD spectra were recorded on a JASCO J-710 spectropolarimeter using quartz cells with path lengths of 0.1 cm. For every set of runs, the CD spectrum of (*R*)-(−)-pantolactone (30 mg in 400 mL of water) was also recorded in a 1 cm cell to ensure reliability of the measurements carried out. All compounds measured were prepared and run more than once, yielding reproducible results. All CD spectra were recorded in Tris buffer (50 mM, pH 8.0, 0.1 M NaCl). The concentrations used were 36 μM for HC_4H_2, 40 μM for HC_4HC, 34 μM for HC_5H, 34 μM for CHC_4H, and 35 μM for all the metallopeptides. The CD spectra reported are the smoothed average of 3−5 scans obtained in 0.5 nm intervals at a rate of 50 nm/min with a response time of 1 s and a bandwidth of 1 nm. Percent helicities were calculated according to the procedure of Chen et al.[44] where the ellipticity at 222 nm for a 100% α-helical peptide of length n is given by $-39\,500[1 - 2.57/n]$ deg·cm^2·dmol^{-1}.

Preparation of $(Me_4N)_2[^{57}Fe_4S_4(SCH_2CH_2OH)_4]$. The literature procedure[39] for the preparation of the unlabeled cluster directly from $NaSCH_2CH_2OH$, $FeCl_3$, and S_8 was slightly modified. Sodium (35 mg, 1.5 mmol) was allowed to react completely with ∼1.5 mL of methanol. The following were then quickly added while stirring: an excess of $HSCH_2CH_2OH$ (1 mL, 14 mmol), a solution of $^{57}FeCl_3$ (from the reaction of 21 mg (0.37 mmol) of ^{57}Fe metal with an excess of HCl at 95 °C) in ∼1.5 mL of methanol, and sulfur (12 mg, 0.37 mmol). The reaction mixture became dark brown in a few minutes. After stirring overnight, the mixture was filtered into a solution of Me_4NBr (39 mg, 0.25 mmol) in ∼2 mL MeOH, stirred for an additional 1 h, and added to ∼30 mL of ether. The precipitates were isolated from the supernatant, washed twice with ether, and dried in vacuo. The desired product was dissolved in ∼7 mL of MeCN with stirring. Finally, the resulting reaction mixture was filtered and layered with ether, producing a total of 12.7 mg (17% yield) of $[Me_4N]_2[^{57}Fe_4S_4(SCH_2CH_2OH)_4]$, pure by ^{1}H NMR.[39]

Preparation of $HC_5H-[^{57}Fe_4S_4]$ and Its Nickel(II) Derivative for Mössbauer Spectroscopy. The procedure for the incorporation of Fe_4S_4 into the 63mer peptides from preformed clusters was followed except that labeled $(Me_4N)_2[^{57}Fe_4S_4(SCH_2CH_2OH)_4]$ was used. The solution of $HC_5H-[^{57}Fe_4S_4]$ obtained through this procedure was concentrated to 300 μM by precipitating with $(NH_4)_2SO_4$, redissolving in a smaller volume of Tris buffer (50 mM, pH 8.0, 0.1 M NaCl), and filtering through a 0.45 μm acrodisc. Once concentrated, a portion of the solution was treated with one equiv of $NiCl_2\cdot 6H_2O$. The two samples were frozen in liquid nitrogen, and their zero-field Mössbauer spectra were recorded on a constant acceleration spectrometer. Data were analyzed using WMOSS software (WEB Research Co., Edina, MN). Isomer shifts are reported with respect to iron metal at room temperature.

(44) Chen, Y.-H.; Yang, J. T.; Chau, K. H. *Biochemistry* **1974**, *13*, 3350−3359.

Other Physical Measurements. Absorption spectra were recorded with a Varian Cary 50 Bio or a Cary 3 spectrophotometer. Atomic absorption experiments were run in a Perkin-Elmer 2380 spectrophotometer.

Results and Discussion

Peptide Design and Synthesis. We seek a peptide scaffold capable of sustaining the assembly $\{Ni^{II}-(\mu_2\text{-}S\cdot Cys)-[Fe_4S_4]^{2+}\}$, containing the metal ion and cluster in normal oxidation states. We have selected cysteinate as bridging group X in view of the well-developed tendency of thiolate sulfur to form bridges in both synthetic systems[45,46] and proteins such as sulfite reductase.[23] Toward this end, we have chosen a helix−loop−helix motif. Each 63mer peptide was designed to incorporate two antiparallel α-helices linked through a loop containing the ferredoxin consensus sequence **Cys**-Ile-Ala-**Cys**-Gly-Ala-**Cys**, in which the cysteinate residues function as cluster ligands. This sequence occurs in *Peptococcus aerogenes* ferredoxin[47] and has been shown to incorporate Fe_4S_4 clusters in synthetic peptides.[4] A fourth cysteine, intended as the bridging group, was positioned toward the *N*-terminus, separated by one residue from the first Cys of the consensus sequence. Even though there are no examples of three-residue **Cys**-Xxa-**Cys** cluster-binding motifs in natural Fe_4S_4 ferredoxins, there is sufficient structural flexibility to allow such binding. The peptide chain chosen for the helical fragments contains the heptad repeat pattern for coiled coils[48] and is analogous to the sequence of other known synthetic α-helices.[4,49−53] Three metal binding residues were inserted inside the helices in positions close to the loop region such that the nickel ion could potentially bind to these residues and one of the cluster-bound cysteinates in a distorted square planar fashion, as in the proposed structure of center A.[31] Specifically, the *N*-terminal helix was provided with a **His**-Xxa-Xxa-Xxa-**Cys** motif, and the *C*-terminal helix with a **His**-Xxa-Xxa-Xxa-**His** motif. The resulting His_3 arrangement has precedence in the design of binding sites for three-coordinate Zn(II) in helix−loop−helix peptides.[54,55] Furthermore, both **His**-Xxa-Xxa-Xxa-**Cys** and **His**-Xxa-Xxa-Xxa-**His** have been shown to bind several metal(II) ions, as shown by Ghadiri and Choi[56] with 17mer peptides containing either the sequence **Cys**-Ala-Ala-Ala-**His** or the sequence **His**-Ala-Ala-Ala-**His**. Additionally, Zn(II) and Co(II) have been bound to a modified 4-helix bundle protein at a binding site containing the **Cys**-Leu-Glu-Glu-**His** motif in one helix and the **Cys**-Leu-Lys-Glu-**His** motif in the adjacent helix.[55,57]

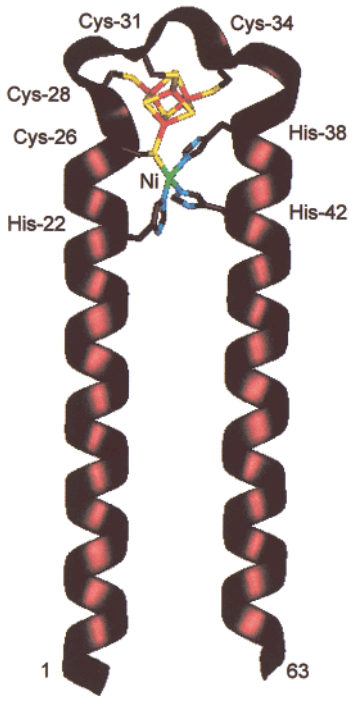

Figure 3. Target $HC_4H_2-[Fe_4S_4]-Ni$ peptide modeled with Quanta.

The α-helices were designed in order to provide a preformed binding site for Ni(II) through intramolecular interaction of the two helices and to prevent formation of oligomers upon addition of a Ni(II) source. Within the hydrophobic pocket, four phenylalanine residues were incorporated to keep enough distance between the two helices to provide space for the nickel ion. Although the nickel atom in center A of CODH is thought to be bound to two sulfur ligands and two nitrogen or oxygen ligands,[31] the first peptide was designed to contain one Cys and three His residues in the nickel binding site to exclude the possibility of a fifth cysteine disrupting the Fe_4S_4 cluster incorporation procedure. Overall, these criteria resulted in the following sequence for the initial 63mer peptide:

Ac-Leu-Lys-Lys-Leu-Lys-Glu-Glu-Phe-Leu-Lys-Leu-Leu-Glu-Glu-Phe-Lys-Lys-Leu-Leu-Glu-Glu-^{22}**His**-Leu-Lys-Leu-^{26}**Cys**-Glu-^{28}**Cys**-Ile-Ala-^{31}**Cys**-Gly-Ala-^{34}**Cys**-Gly-Gly-Glu-^{38}**His**-Leu-Lys-Leu-^{42}**His**-Glu-Glu-Leu-Leu-Lys-Lys-Phe-Glu-Glu-Leu-Leu-Lys-Leu-Phe-Glu-Glu-Lys-Leu-Lys-Lys-Leu-$CONH_2$.

Three variants of this sequence were then prepared in search of ligand environments that would (i) resemble that of the nickel ion in center A of the enzyme more closely (i.e., an N_2S_2 ligand environment) and (ii) bind Ni(II) more tightly. Presented in Figure 2 are the chosen variants His42Cys, His38Cys, and Cys26His/His22Cys/His38Cys. These are hereafter designated according to the sequence of their metal binding residues starting from their *N*-terminus as HC_4HC, HC_5H, and CHC_4H, respectively. Likewise, the original 63mer is HC_4H_2. Molecular modeling of the target metallopeptides was performed using QUANTA, and the structures were refined with CHARMm. The modeled target $HC_4H_2-[Fe_4S_4]-Ni$ metallopeptide is schematically depicted in Figure 3 .

All 63mers were successfully synthesized and purified as shown by the analytical HPLC chromatograms in Figure 4 and the ES-MS of the purified peptides, exemplified by the spectrum of HC_4H_2 in Figure 5. Characterization data for the four 63mers and their metalloderivatives are collected in Table 1.

(45) Blower, P. J.; Dilworth, J. R. *Coord. Chem. Rev.* **1987**, *76*, 121−185.
(46) Krebs, B.; Henkel, G. *Angew. Chem., Int. Ed. Engl.* **1991**, *30*, 769−788.
(47) Adman, E. T.; Sieker, L. C.; Jensen, L. H. *J. Biol. Chem.* **1973**, *248*, 3987−3996.
(48) Betz, S. F.; Bryson, J. W.; DeGrado, W. F. *Curr. Opin. Struct. Biol.* **1995**, *5*, 457−463.
(49) Robertson, D. E.; Farid, R. S.; Moser, C. C.; Urbauer, J. L.; Mulholland, S. E.; Pidikiti, R.; Lear, J. D.; Wand, A. J.; DeGrado, W. F.; Dutton, P. L. *Nature* **1994**, *368*, 425−432.
(50) Rabanal, F.; DeGrado, W. F.; Dutton, P. L. *J. Am. Chem. Soc.* **1996**, *118*, 473−474.
(51) Gibney, B. R.; Rabanal, F.; Skalicky, J. J.; Wand, A. J.; Dutton, P. L. *J. Am. Chem. Soc.* **1997**, *119*, 2323−2324.
(52) Gibney, B. R.; Johansson, J. S.; Rabanal, F.; Skalicky, J. J.; Wand, A. J.; Dutton, P. L. *Biochemistry* **1997**, *36*, 2798−2806.
(53) Gibney, B. R.; Rabanal, F.; Reddy, K. S.; Dutton, P. L. *Biochemistry* **1998**, *37*, 4635−4643.
(54) Handel, T.; DeGrado, W. F. *J. Am. Chem. Soc.* **1990**, *112*, 6710−6711.
(55) Handel, T. M.; Williams, S. A.; DeGrado, W. F. *Science* **1993**, *261*, 879−885.
(56) Ghadiri, M. R.; Choi, C. *J. Am. Chem. Soc.* **1990**, *112*, 1630−1632.
(57) Regan, L.; Clarke, N. D. *Biochemistry* **1990**, *29*, 10878−10883.

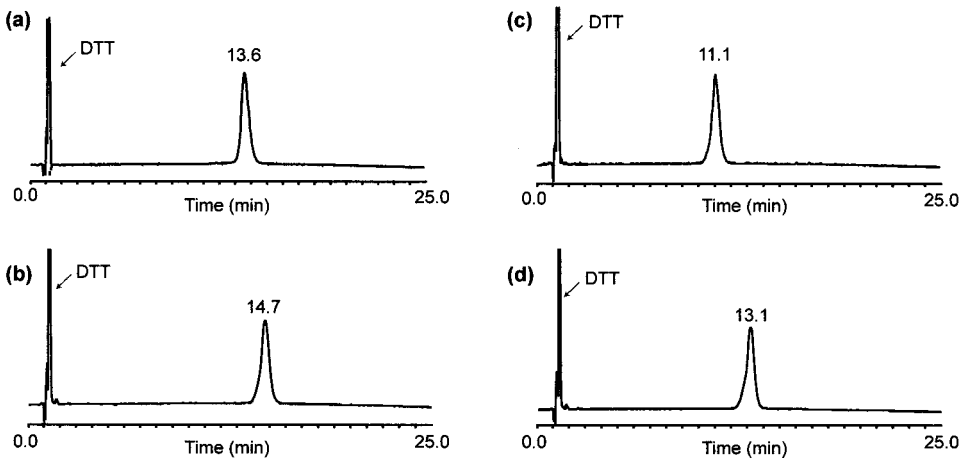

Figure 4. Analytical reversed-phase HPLC chromatograms of purified HC_4H_2 (a), HC_4HC (b), HC_5H (c), and CHC_4H (d) using linear gradients over 25 min of CH_3CN/0.1% TFA in H_2O/0.1% TFA at a flow rate of 1.3 mL/min from 30 to 70% for (a) and from 35 to 75% for (b), (c), and (d).

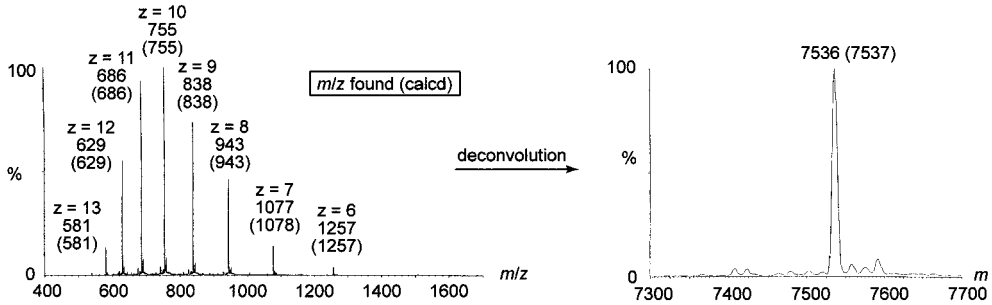

Figure 5. ES-MS spectrum of purified HC_4H_2−peptide and its deconvoluted molecular weight spectrum. Theoretical *m*/*z* values are given in parentheses.

Fe_4S_4 Incorporation. In all peptides, the incorporation of the Fe_4S_4 cluster could be accomplished by reaction with $(Me_4N)_2[Fe_4S_4(SCH_2CH_2OH)_4]$. The UV−vis spectra shown in Figure 6a reveal the charge-transfer bands typical of an $[Fe_4S_4]^{2+}$ cluster at 390 and 280 nm in the expected intensity ratios, providing no indication for the existence of any other iron species. The zero-field Mössbauer spectrum collected on $HC_5H-[^{57}Fe_4S_4]$ at 4.2 K (Figure 7a) exhibits a symmetric quadrupole doublet with quadrupole splitting $\Delta E_Q = 1.13$ mm/s and an isomer shift $\delta = 0.45$ mm/s which is entirely consistent with the $[Fe_4S_4]^{2+}$ oxidation level.[58] Therefore, to determine the ratio Fe_4S_4:peptide in each sample, all the iron detected by atomic absorption was assumed to be in the form of an Fe_4S_4 cluster. The validity of this assumption is further supported by the extinction coefficients calculated for the bands at 290 nm (22 000−23 100 $M^{-1}cm^{-1}$) and 380 nm (16 100−17 300 $M^{-1}cm^{-1}$), which are consistent with those reported for Fe_4S_4-ferredoxins[59] and $[Fe_4S_4(SCH_2CH_2OH)_4]^{2-}$ in aqueous solution.[38] The peptide concentration was calculated on the basis that all the peptide present at the beginning of the reaction was recovered after column chromatography. Under these premises, ratios of 0.85−0.95 Fe_4S_4 cluster per 63mer peptide have been consistently obtained.

Incorporation of Ni(II). After addition of 1 equiv of $NiCl_2 \cdot 6H_2O$ to each 63mer-$[Fe_4S_4]$, Sephadex column chromatography was performed to remove any peptide-free nickel ions. Atomic absorption analysis of the eluant revealed different Fe:Ni ratios of 4Fe:0.5−0.8 Ni depending on the peptide and the length of the column used for purification. The Mössbauer spectrum of Ni(II)-treated $HC_5H-[Fe_4S_4]$ (Figure 7b) shows that approximately 90% of the iron is still in the form of $[Fe_4S_4]^{2+}$, while the remaining appears to be in the form of high spin Fe(II), probably due to decomposition of the cluster during the handling of the sample.

The product of $CHC_4H-[Fe_4S_4]$ with $NiCl_2 \cdot 6H_2O$ yielded UV−vis, EXAFS,[60] and nickel binding data inconsistent with the desired target metallopeptide. The Ni(II) coordination unit has not been identified; consequently, this metallopeptide is not discussed further. The absorption spectra of the remaining three 63mer−$[Fe_4S_4]$−Ni peptides show additional absorption (Figure 6b) that, as explained below, can be attributed to LMCT contributions arising from the presence of a Ni−S•Cys moiety. This effect causes the well-defined features at 290 and 380 nm originating from the $[Fe_4S_4]^{2+}$ cluster to be partially obscured as shoulders.

Subtraction of the appropriate 63mer−$[Fe_4S_4]$ absorption spectrum from the spectra obtained in metallopeptide samples equilibrated for 20 h with 0.56 and 1.1 equiv of $NiCl_2 \cdot 6H_2O$ resulted in the difference spectra presented in Figure 6c−e. These spectra show featureless absorption in the 400−700 nm region, likely owing to unresolved d−d transitions, in addition to a band at 260 nm and a shoulder at 320 nm, the last two suggesting that Ni(II) has thiolate ligation. Detection of nickel by atomic absorption after column chromatography provides a positive indication that Ni(II) is binding to the metallopeptide, thus Ni(II) must coordinate one or more cysteinate residues. After 1.1 equiv of Ni(II), the extinction coefficients for the 260

(58) Bertini, I.; Ciurli, S.; Luchinat, C. *Struct. Bonding (Berlin)* **1995**, *83*, 1−53.

(59) Hong, J.-S.; Rabinowitz, J. C. *J. Biol. Chem.* **1970**, *245*, 4982−4987.

(60) Musgrave, K. B.; Laplaza, C. E.; Holm, R. H.; Hedman, B.; Hodgson, K. O. Unpublished results.

Table 1. Characterization Data for 63Mer Peptides and Their Metalloderivatives

		HC_4H_2	HC_4HC	HC_5H	CHC_4H
apopeptides	ES-MS mass found (calcd)[a]	7536 (7537)	7498 (7498)	7496 (7498)	7499 (7498)
	SEC[b] mass found (calcd for the dimer)[c]	18.0 (15.1)	18.4 (15.0)	18.5 (15.0)	18.4 (15.0)
	CD[b] helicity,[d] $\theta_{222}/\theta_{209}$	75%, 1.10	74%, 1.04	69%, 1.08	75%, 1.07
63mer−$[Fe_4S_4]$−peptides	UV−vis[b] λ_{max} (ϵ_M)[e]	290 (22 000 ± 800) 380 (16 300 ±500)	290 (22 600 ± 400) 380 (16 500 ±300)	290 (23 100 ± 800) 380 (17 300 ±500)	290 (22 100 ± 600) 380 (16 100 ±500)
	Mössbauer ΔE_Q,[f] δ[f]			1.13, 0.45	
	SEC[b] mass found[c] (molecularity)	19.3 (2.4) 43.4 (5.5) 55.9 (7.1)	24.6 (3.1) 29.6 (3.8) 50.9 (6.5) 65.9 (8.4)	22.6 (2.9) 28.2 (3.6) 50.0 (6.4) 63.8 (8.1)	21.7 (2.8) 25.7 (3.3) 46.5 (5.9) 58.8 (7.5)
	CD[b] helicity,[d] $\theta_{222}/\theta_{209}$	70%, 1.00	50%, 1.01	60%, 1.00	58%, 1.01
63mer−$[Fe_4S_4]$− peptides + 1 equiv of $NiCl_2{\cdot}6H_2O$	UV−vis[b] λ_{max} (ϵ_M)[e]	290 (23 400 ± 700) 380 (16 300 ± 500)	290 (26 300 ± 400) 380 (17 400 ± 100)	290 (26 800 ± 1800) 380 (18 300 ± 1600)	*g*
	Mössbauer ΔE_Q,[f] δ[f]			1.13, 0.46	
	CD[b] helicity,[d] $\theta_{222}/\theta_{209}$	69%, 0.96	52%, 0.99	58%, 0.97	

[a] Da. [b] In Tris buffer (50 mM, pH 8.0, 0.1 M NaCl). [c] kDa. [d] Approximately ±5%. [e] nm ($M^{-1}cm^{-1}$); ϵ_M per monomeric 63mer$[Fe_4S_4]$ component; errors reported at the 95% confidence interval. [f] mm/s, at 4.2 K. [g] Data obtained are inconsistent with desired metallopeptide; product has not been identified.

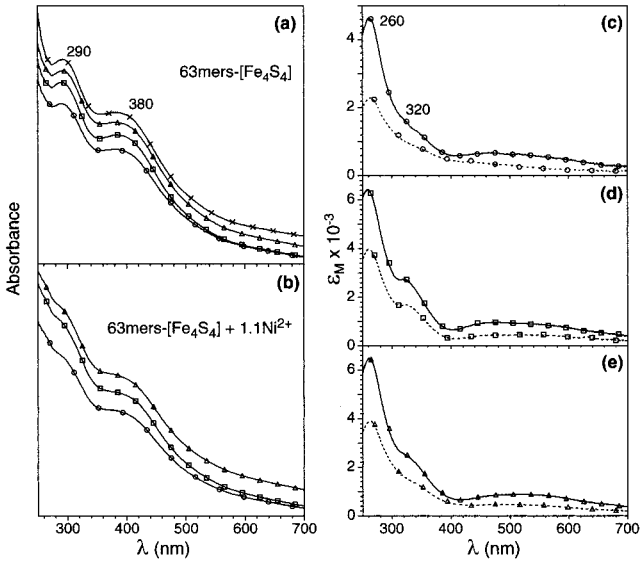

Figure 6. Absorption spectra of (a) 63mers−$[Fe_4S_4]$ and (b) 63mers−$[Fe_4S_4]$ after equilibration with 1.1 equiv of $NiCl_2{\cdot}6H_2O$. The traces have been offset for clarity of the absorption bands. ○ represents the HC_4H_2 metalloderivatives; □, HC_4HC; △, HC_5H; and ×, CHC_4H. The extinction coefficients are given in Table 1. (c)−(e) Difference spectra resulting from the subtraction of the absorption of (c) HC_4H_2−$[Fe_4S_4]$, (d) HC_4HC−$[Fe_4S_4]$, and (e) HC_5H−$[Fe_4S_4]$ from the appropriate spectra of the Ni-containing metallopeptides, after equilibrium with 0.56 equiv of $NiCl_2{\cdot}6H_2O$ (dashed line) and 1.1 equiv of $NiCl_2{\cdot}6H_2O$ (solid line).

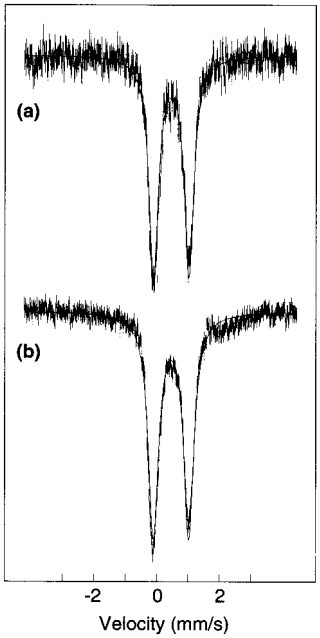

Figure 7. Zero-field spectra collected at 4.2 K of (a) HC_5H−$[^{57}Fe_4S_4]$ and (b) HC_5H−$[^{57}Fe_4S_4]$ after the addition of 1 equiv of $NiCl_2{\cdot}6H_2O$. The solid lines drawn through the experimental data represent quadrupole doublets with (a) $\Delta E_Q = 1.13$ mm/s and $\delta = 0.45$ mm/s and (b) $\Delta E_Q = 1.13$ mm/s and $\delta = 0.46$ mm/s.

and 320 nm bands are, respectively, 4600 $M^{-1}cm^{-1}$ and 1600 M^{-1} cm^{-1} for the HC_4H_2−metallopeptide, ∼6400 $M^{-1}cm^{-1}$ and ∼2700 $M^{-1}cm^{-1}$ for the HC_4HC−metallopeptide, and ∼6500 $M^{-1}cm^{-1}$ and ∼2500 $M^{-1}cm^{-1}$ for the HC_5H−metallopeptide. These extinction coefficients are per monomeric 63mer−$[Fe_4S_4]$ unit, and they arise from a species containing less than 1 equiv of peptide-bound Ni per 63mer−$[Fe_4S_4]$ unit, as nickel appears to be distributed between a free form, presumably $[Ni(H_2O)_6]^{2+}$, and a peptide-bound form. Evidence for this distribution includes (i) loss of nickel on column chromatography, with further loss upon running a second columnn, (ii) nickel binding studies,[61]

(61) Laplaza, C. E.; Holm, R. H. Results to be published.

Table 2. Experimental and Actual Masses of Four-Helix Bundles

	masses (kDa)		
	actual	exptl	ref
cytochrome b_{562}	12.3	18.1	67
Rau and Haehnel's synthetic four-helix bundle protein	14.3	18.6	5
Rau and Haehnel's synthetic bis-heme four-helix bundle protein	15.5	18.8	5
Dutton and co-workers' $\{[H10H24]_2\}_2$	15.2	20.1	53
$[HC_4H_2]_2$	15.1	18.0	this work
$[HC_4HC]_2$	15.0	18.4	this work
$[HC_5H]_2$	15.0	18.5	this work
$[CHC_4H]_2$	15.0	18.4	this work

and (iii) EXAFS results.[62] Preliminary analysis of the nickel binding data suggests that there are multiple binding sites for the nickel in the three metallopeptides, including 1 strong site per monomeric units of $HC_4H_2-[Fe_4S_4]$ and $HC_5H-[Fe_4S_4]$, and 0.5 strong site per $HC_4HC-[Fe_4S_4]$ unit, that is, 1 strong site per $\{HC_4HC-[Fe_4S_4]\}_2$. All other binding sites in the metallopeptides are much weaker and thus are not meaningful. That only 0.5 equiv of strong sites is found per $HC_4HC-[Fe_4S_4]$ unit is consistent with the suggestion originating from CD studies (vide infra) that the Fe_4S_4 cluster binds Cys42 as opposed to Cys26, a scenario in which nickel does not have a preformed binding site.

Consistent with the EXAFS results,[62] the positions and intensities of the absorption bands in the difference spectra of Figure 6c−e, where the extinction coefficients refer to species with <1 equiv of Ni(II) in the desired binding site,[61] resemble more closely those of distorted square planar Ni(II) complexes than those of distorted tetrahedral Ni(II) complexes. Examples of the former with peptidic ligands include a recently reported tetracysteinyl cyclopeptide nickel(II) complex,[63] which shows a UV−vis spectrum with λ_{max} (ϵ_M) = 295 (∼13 500), 335 (∼10 000), 420 (sh, ∼3500), and 630 (sh, ∼400) nm and a Cys_2-His_2-peptide nickel(II) complex[64] with features at 328 (5700), 410 (sh, 720), and 500 (sh, 300) nm. Distorted tetrahedral nickel(II) complexes with a Cys_2His_2 coordination site include a finger peptide prepared by Krizek and Berg[65] with bands at 310 (∼2200), 360 (∼2200), 400 (∼2500), 550 (∼150), and 650 (∼150) nm, and a finger peptide prepared by Posewitz and Wilcox[66] with features at 305 (∼1900), 380 (∼1300), 400 (sh, ∼1100), 525 (∼100), and 625 (∼50). Altogether, the absorption spectra of the Ni-containing 63mer-metallopeptides together with nickel binding studies[61] and the EXAFS[62] of $HC_4H_2-[Fe_4S_4]$−Ni and $HC_5H-[Fe_4S_4]$−Ni strongly indicate that Ni(II) binds to the desired His_3Cys and His_2Cys_2 sites, respectively.

Size-Exclusion Chromatography of Peptides and Metallopeptides. Apparent molecular weights were determinated by this technique. The four peptides in Figure 2 afforded the experimental masses of 18.0−18.5 kDa presented in Table 2. These values are 3.0−3.5 kDa greater than the expected masses of 15.1 kDa for $[HC_4H_2]_2$ and 15.0 kDa for each of the variant dimers. This disparity is not surprising, as the standards used to calibrate the size-exclusion chromatography column are globular proteins, while the 63mer peptides are cylindrical and thus expected to elute faster than if they were globular. As shown in Table 2, the differences observed herein are comparable to peptides of the same mass that are known to exist as four-helix bundles such as cytochrome b_{562},[67] Rau and Haehnel's synthetic four-helix bundle protein and bis-heme derivative,[5] synthetic four-helix bundles reported by Dutton and co-workers,[49,53] and related helical peptides.[49,52,53] Accordingly, we conclude that the four 63mer peptides are largely or completely dimeric with a four-helix bundle structure. The relative orientation of the two helix−loop−helix fragments about each other is not known at this point.

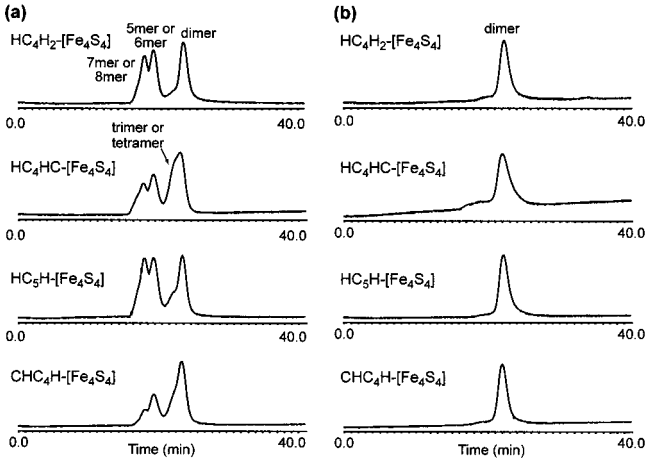

Figure 8. Size-exclusion chromatography traces of the indicated 63mer−$[Fe_4S_4]$ peptides in (a) Tris buffer (50 mM, pH 8.0, 0.1 M NaCl) and in (b) 20% TFE/80% Tris buffer.

Upon Fe_4S_4 incorporation, size-exclusion chromatography revealed the presence of several aggregates (Figure 8a) in the concentration range studied (50−100 μM). The molecularity corresponding to each of these aggregates could not be assigned with certainty, because their shapes are unknown. However, in the presence of 20% trifluoroethanol (v/v), all higher aggregates broke down into dimers (Figure 8b), while absorption spectra showed that the Fe_4S_4 clusters remained intact. Had these higher aggregates been cross-linked species (in which clusters are bound to more than one peptide), it should not have been possible to break them down without destroying the cluster. Identical size-exclusion chromatography results (not shown) have been obtained upon the addition of 1 equiv of Ni(II).

In search of evidence against cross-linking within the metallopeptide dimers, we have first sought conditions under which peptides themselves are monomeric. Increasing concentrations of trifluoroethanol, a frequently used method of peptide dissociation, has thus far yielded inconclusive results.

Circular Dichroism Spectropolarimetry of Peptides and Metallopeptides. As seen in Figure 9, the CD spectra of all 63mer peptides and metallopeptides exhibit a strong negative feature at 209 nm and another band at 222 nm, both of which are typical of α-helices.[68] The molar ellipticities at 222 nm show that all peptides except HC_5H are approximately 75% helical (Figure 9a). The slightly lower helicity of HC_5H is not significant and is within the errors of the measurement. The ratios $\theta_{222}/\theta_{209} > 1$ exhibited by the peptides have been suggested to be diagnostic of coiled coil structures.[69−71] However, because Holtzer and Holtzer[72] have shown that this criterion is not reliable for differentiating coiled coils from single α-helices, this aspect of the CD spectra is not analyzed here.

(62) Musgrave, K. B.; Laplaza, C. E.; Holm, R. H.; Hedman, B.; Hodgson, K. O. Submitted for publication.

(63) Nivorozhkin, A. L.; Segal, B. M.; Musgrave, K. B.; Kates, S. A.; Hedman, B.; Hodgson, K. O.; Holm, R. H. *Inorg. Chem.* **2000**, *39*, 2306−2313.

(64) Bal, W.; Lukszo, J.; Jezowska-Bojczuk, M.; Kasprzak, K. S. *Chem. Res. Toxicol.* **1995**, *8*, 683−692.

(65) Krizek, B. A.; Berg, J. M. *Inorg. Chem.* **1992**, *31*, 2984−2986.

(66) Posewitz, M. C.; Wilcox, D. E. *Chem. Res. Toxicol.* **1995**, *8*, 1020−1028.

(67) Feng, Y.; Sligar, S. G. *Biochemistry* **1991**, *30*, 10150−10155.

(68) *Circular Dichroism and the Conformational Analysis of Biomolecules*; Fasman, G. D., Ed.; Plenum Press: New York, 1996.

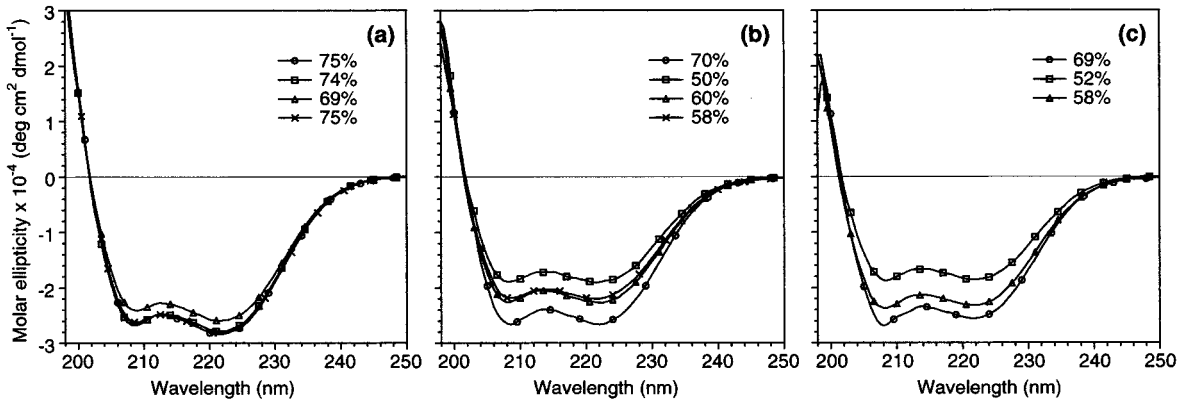

Figure 9. Circular dichroism spectra of (a) 63mer peptides, (b) 63mers−$[Fe_4S_4]$, and (c) 63mers−$[Fe_4S_4]$ after addition of 1 equiv of $NiCl_2{\cdot}6H_2O$. ○ represents HC_4H_2 and its metalloderivatives; □, HC_4HC; △, HC_5H; and ×, CHC_4H. Helical contents are given above for each species.

Upon Fe_4S_4 cluster incorporation, the helical content of the metallopeptides decreases relative to their respective 63mers to 70% in HC_4H_2−$[Fe_4S_4]$, 60% in HC_5H−$[Fe_4S_4]$, 58% in CHC_4H−$[Fe_4S_4]$, and 50% in HC_4HC−$[Fe_4S_4]$ (Figure 9b). After addition of 1 equiv of Ni(II) and a 20-hour equilibration, the helicities of the resulting metallopeptides (Figure 9c) were virtually the same as those found for their respective 63mer−$[Fe_4S_4]$ precursors. Further, the use of *2* equiv of Ni(II), a condition under which more of the nickel binding sites are occupied, did not cause any changes in the helical contents of the metallopeptides. We conclude that the peptide design has yielded the desired 63mer−$[Fe_4S_4]$ species with a preformed binding site for Ni(II). The lower helical contents found in the HC_4HC metallopeptides suggest that the Fe_4S_4 cluster binds to Cys42, and not to Cys26. This implication constitutes a putative example of the binding selectivity of the Fe_4S_4 cluster for the Cys residue located toward the peptide *C*-terminus over the Cys residue positioned toward the *N*-terminus. Interestingly, the fourth cysteine that binds the Fe_4S_4 cluster in natural 4-Fe-ferredoxins is found toward the *C*-terminus, after the consensus sequence **Cys**-Xxa-Xxa-**Cys**-Xxa-Xxa-**Cys**.[73]

Assuming that the former premise is indeed correct, then the overall trend found for the helical contents of the metallopeptides correlates with the length of the peptidic fragment wrapping around the Fe_4S_4 cluster. The HC_4H_2 metallopeptides, containing the smallest Fe_4S_4 binding loops of 9 residues, show the highest helicities (70%) of all metallopeptides. The lowest helical content of 50% is found for the HC_4HC metallopeptides which appear to contain the longest Fe_4S_4 binding loops of 15 residues. If the preference of the Fe_4S_4 cluster for binding the cysteine toward the *C*-terminus remains in the HC_5H and CHC_4H metallopeptides, their Fe_4S_4 binding loop length of 11 residues corresponds well with the experimentally found intermediate helical contents of 60%.

Summary and Conclusions. We have synthesized and purified four 63mer peptides which are designed to sustain the bridged assembly [Ni−X−Fe_4S_4] that may be present in center A of CODH. Each monomeric helix−loop−helix component was designed to bind an $[Fe_4S_4]^{2+}$ cluster by means of a ferredoxin consensus sequence introduced in the loop. A nearby N_3S or N_2S_2 site, intended to bind a Ni(II) atom with concomitant bridging to the Fe_4S_4 cluster through a cysteinate sulfur atom, was introduced by appropriate placement of histidine and cysteine residues near the loop (Figure 2). Convincing evidence for the incorporation of an Fe_4S_4 cluster in each peptide follows from absorption spectra, Mössbauer spectra, and iron EXAFS.[62] Together with iron atomic absorption analysis, these data demonstrate that each 63mer fragment binds one $[Fe_4S_4]^{2+}$ cluster. Evidence for the incorporation of Ni(II) includes nickel atomic absorption after Sephadex column chromatography which shows that nickel is binding to the metallopeptide while in an apparent equilibrium with free Ni(II). Nickel EXAFS[62] of HC_4H_2−$[Fe_4S_4]$−Ni and HC_5H−$[Fe_4S_4]$−Ni corroborates the existence of this equilibrium in these two metallopeptides and, further, provides strong evidence that peptide-bound Ni(II) is in the desired N_3S or N_2S_2 site according to the variant.

Size-exclusion chromatography indicates the four 63mers are dimeric in solution. The relative orientation of the individual peptides within these four-helix bundles remains elusive. However, preliminary EXAFS data on HC_5H−$[Fe_4S_4]$ treated with sodium dithionite reveals that the cluster does not remain intact and shows long-range scattering interactions.[60] We speculate that upon reduction the two $[Fe_4S_4]^{2+}$ clusters of the dimer might rearrange into one larger cluster, hinting that the dimer structure must entail two helix−loop−helix 63mer peptides oriented parallel to each other. However, we have been unable to draw structural conclusions from the Mössbauer or EPR spectra of the reduced metallopeptides.

Of the numerous metallopeptide syntheses previously reported, this research is most closely related in intent to those cases, limited in number, in which peptides are designed to bind more than one metal cofactor. Examples include multi-ruthenium-containing peptides,[3,6,74] Ghadiri's heterodinuclear $Ru^{II}Cu^{II}$ three-helix bundle metalloprotein,[75] the maquette of Dutton and co-workers[4] that binds four hemes and two Fe_4S_4 clusters, synthetic four-helix bundles that bind two or four hemes,[49,50,52,53] the cytochrome *b* model of Rau and Haehnel[5] that also binds two hemes, the synthetic clostridial ferredoxins of Feinberg and co-workers[13,14,16] that contain two Fe_4S_4 clusters, and the dimetal four-helix bundles of DeGrado and co-workers.[21] In the first six examples, the metal-containing units are not covalently linked to each other. DeGrado and co-workers' dimetal peptides find a relation with this work in that they were designed to bridge two metal sites, accomplished by the unit M(μ_2-η^1:η^1-

(69) Lau, S. Y. M.; Taneja, A. K.; Hodges, R. S. *J. Biol. Chem.* **1984**, *259*, 13253−13261.
(70) Zhou, N. E.; Kay, C. M.; Hodges, R. S. *Biochemistry* **1992**, *31*, 5739−5746.
(71) Zhou, N. E.; Kay, C. M.; Hodges, R. S. *J. Biol. Chem.* **1992**, *267*, 2664−2670.
(72) Holtzer, M. E.; Holtzer, A. *Biopolymers* **1995**, *36*, 365−379.
(73) Matsubara, H.; Saeki, K. *Adv. Inorg. Chem.* **1992**, *38*, 223−280.
(74) Dahiyat, B. I.; Meade, T. J.; Mayo, S. L. *Inorg. Chim. Acta* **1996**, *243*, 207−212.
(75) Ghadiri, M. R.; Case, M. A. *Angew. Chem., Int. Ed. Engl.* **1993**, *32*, 1594−1597.

Glu·CO_2)$_2$M as determined by the X-ray structure of the dizinc derivative. In the present systems, the desired bridge is [Ni−(μ_2-S·Cys)−Fe]. XAS (X-ray absorption spectroscopy) data[62] and the detailed characterization of four 63mers and their metalloderivatives provide further support for the idea that designed peptides can act as scaffolds in the stabilization of assemblies containing two metal components in close proximity, in a manner intended to represent a native protein-bound site. Whether the spectroscopically based structural description of the A-cluster of CODH is correct is less the issue here than its value as a structural and reactivity objective, and, therewith, a test of the scaffolding concept. X-ray absorption spectroscopic results bearing on structural features of the metal sites will be reported separately,[62] as will other aspects of the metal binding properties of the 63mer peptides.[61]

Acknowledgment. This research was supported by NIH Grant GM 28856. We are grateful to Dr. S. A. Kates (Consensus Pharmaceuticals, Medford, MA) and J. F. McNamara (Applied Biosystems, Framingham, MA) for use of equipment, experimental assistance, and helpful discussion. C.E.L. has been the recipient of a NSF Minority Graduate Fellowship and a Harvard University Graduate School of Arts and Sciences Graduate Prize Fellowship.

Note Added in Proof. The structure of *Carboxydothermus hydrogenofomans* CODH has been recently solved at 1.6 Å resolution: Dobbek, H.; Svetlitchnyi, V.; Gremer, L.; Huber, R.; Meyer, O. *Science* **2001**, *293*, 1281−1285. Active site center C deviates from the spectroscopic model. It has the $NiFe_4S_5$ core composition in which the Ni atom is bonded to two sulfur atoms of a cuboidal Fe_3S_4 fragment and bridged through an Ni−S−Fe interaction to a Fe atom external to this fragment.

JA010851M